Covariant cubic approximation for many-body electronic systems

Baruch Rosenstein[1,*] and Dingping Li[2,3,†]

[1]*Electrophysics Department, National Chiao Tung University, Hsinchu 30050, Taiwan, Republic of China*
[2]*School of Physics, Peking University, Beijing 100871, China*
[3]*Collaborative Innovation Center of Quantum Matter, Beijing 100871, China*

An approximation scheme determining the excitations of an electronic model on the lattice with pairwise interactions is proposed. A systematic truncation of the set of Dyson-Schwinger equations for correlators, supplemented by a "covariant" calculation of correlators lead to a converging series of approximates. The covariance preserves all the Ward identities among correlators describing various condensed matter probes. It is shown that the third-order approximant of this kind beyond classical and Gaussian (Hartree-Fock) is precise enough and due to several fortunate features the complexity of calculation is surprisingly low so that a realistic material computation might be feasible. Focus here is on the electron field correlator describing the electron (hole) excitations measured in photoemission and other probes. The scheme is tested on several solvable benchmark models.

I. INTRODUCTION

Calculation of the band structure and response functions of crystalline material with determined chemical composition is one of the most important theoretical problems in condensed matter physics. However, computing the electronic excitations and spectra of a stoichiometric chemically well-defined compounds with significant correlations from first-principles continues to be a major challenge in computational material science. Historically, the Kohn-Sham density functional method [1] (DFT) opened the door to such calculations. The method approximates the many-body physics by noninteracting electrons in a periodic potential. It is successful to map out general features of the band structure of numerous crystalline solids.

However, DFT is not accurate enough in the most important (for condensed matter physics) range of energies near the Fermi level for which many-body effects are important. Kohn-Sham eigenvalues have been used to interpret the single-particle excitation energies measured in direct and inverse photoemission experiments. Reasonable results were obtained in simple metals, however, when the excited state properties of semiconductors and insulators are concerned, ambiguities between different DFT approaches (for example, the exchange correlation functional) and significant deviations from the measured characteristics appear.

In order to tackle the problem of DFT, the many-body-theory-based methodologies were applied to condensed-matter physics recently by including the correlation effects. For example, the dynamical mean field theory [2], Hedin's GW approximation [3], and diagrammatic fluctuational exchange [4] were developed. A particularly troublesome problem for various extensions is that the result must respect basic conservations like the charge conservation. Hybertsen and Louie [5] showed that applying GW approximation as a first-order perturbation to the Kohn-Sham quasiparticles (so-called G_0W_0) provides an improved description of the photoemission spectra described by the electron Greens function.

However, it is known that the method violates conservation laws. The self-consistent GW (scGW) does better. It belongs to the class of the so-called Φ-derivable approximations [6]. It was shown [7] that for these schemes expectation values of Noether currents (like electric current, momentum, etc.) are conserved. The scGW was applied to various systems [8] including to crystalline solids [9]. However, scGW still significantly overestimates the bandwidth for metals and band gaps for insulators. This might be attributed to the violation of the Ward identities of the scGW approximation. While in Φ-derivable approximations like scGW the expectation values of Noether currents are conserved, general Ward-Takahashi identities (WTI) are not guaranteed [10]. For example, Kutepov demonstrated, using the two-site Hubbard model, that certain vertex corrections ($G\Gamma_1W$ in Ref. [11]) to scGW reduce the WTI violation's level. Recent scGW calculations incorporating the vertex correction demonstrated a substantial improvement to the bandwidths, ionization potential, and the band gaps of crystalline materials compared to the original scGW [12,13]. There exist alternative approaches. For example, WTI is *imposed* by construction (not a self-consistent approach) in Ref. [14].

A general method to preserve the WTI in an approximation scheme was developed long time ago [15] in the context of field theory as the covariant Gaussian approximation (CGA) to solve an unrelated problem in quantum field theory and superfluidity [16]. A nonperturbative variational Gaussian method which originated in the quantum mechanics of atoms and molecules in relativistic theories like the standard model of particle physics had several serious related problems. First,

*baruchro@hotmail.com
†lidp@pku.edu.cn

the wave function renormalization required a dynamical description. Second, the Green's functions obtained using the naive Gaussian approximation violated the charge conservation. In particular, the most evident problem is that the Goldstone bosons that resulted from spontaneous breaking of continuous symmetry are massive. The method is thus considered dubious and or inconsistent. Both problems were solved by an observation that the solution of the minimization equations is not necessarily equivalent to the variational Green's function. This constitutes the covariant Gaussian approximation or CGA [15].

The method was compared with available exact results for the S matrix in the Gross-Neveu model [17] (a local four-fermion interaction in 1D Dirac excitations recently considered in condensed matter physics) and with MC simulations in various scalar models, see Ref. [18] for detailed description and application to thermal fluctuations in superconductors in the framework of the Ginzburg-Landau-Wilson order parameter approach [19]. Applied to the electronic field correlator in electronic systems, CGA becomes roughly equivalent to the Hartree-Fock (HF) approximation, which is generally not precise enough—its covariance might improve the calculation of the four-fermion correlators like the density-density, but to address quantitatively photoemission or other direct electron or hole excitation probes, a more precise method is needed.

The CGA approach is just the second in a sequence of approximations based on covariant truncations of the Dyson-Schwinger (DS) equations in which cumulant of third and higher orders are discarded. One can continue to the next level by retaining the third cumulant (discarding the fourth), etc. We term this approximation covariant cubic approximation, CCA. The covariance still preserves all the Ward identities. Up to now, the methodology of this kind has not been applied to more microscopic description of realistic condensed matter systems.

The subject of the present paper is to inquire whether is possible and computationally feasible. It is shown using several solvable benchmark models, that the third-order approximation that we term a "cubic covariant approximation" (CCA) is precise enough. Its complexity when applied to a realistic material calculation is estimated in the end of the present paper. The focus is on the electron (hole) excitations correlator described by the electron field correlator. Recently, the correlator is being "measured" rather directly by various photo-emission probes like ARPES-angle resolved photoemission spectroscopy. This is especially important for novel clean crystalline materials, many of them low-dimensional semiconductors and the so-called Weyl semimetals, like two-dimensional hexagonal boron nitride (hBN), graphene, etc. Higher correlators like the density-density (or conductivity) can be also calculated using the covariant approximation as shown in Refs. [15,18]. In the present paper, no attempt is made to apply the method to realistic materials, only to the Hubbard model, however, the computational complexity of real materials is estimated.

The paper is organized as follows. In Sec. II, the sequence of covariant approximations developed using the simplest possible case: the one-dimensional integral. Next, in Sec. III, the third approximation of these series, CCA is applied to a (Z_2 invariant) statistical Ginzburg-Landau-Wilson model

[20] describing various statistical mechanical systems like the Ising chain in terms of low-energy (effective) bosonic field theory. The results are compared with exact (at low dimension) and MC simulations (higher dimensionality). In Sec. IV, the general formalism for a downfolded electronic system describing crystalline materials is presented and applied in Sec. V to some low-dimensional benchmark systems like the single-band Hubbard model. Section VI contains an estimate of complexity of application of CCA to a realistic material and conclusions.

II. HIERARCHY OF CONSERVING TRUNCATIONS OF DS EQUATIONS

The main ideas behind the covariant approximants are presented in this section in the simplest possible setting. Later, the third in a series of such approximants for a many-body system will be considered in some detail.

A. An exactly solvable "bosonic" model: one-dimensional integral

To clearly present the general covariant approximation scheme, we will make use of the simplest nontrivial model: the statistical physics of a one-dimensional classical chain that is equivalent to the quantum mechanics of the anharmonic oscillator in the next section. Our starting point here will be the following "free energy" as a function of a single (real) variable ψ:

$$f = \frac{a}{2}\psi^2 + \frac{b}{4}\psi^4 - J\psi. \tag{1}$$

Here, a and b represent spectrum and "couplings," respectively, while the "source" or "external field" J will be used to calculate correlations. The exact partition function of just one "fluctuating" bosonic variable is [21]

$$Z[J] = \int_{\psi=-\infty}^{\infty} e^{-f} = e^{-F[J]}. \tag{2}$$

Correlators (Green's function) are defined as

$$G_n = \frac{d^n}{dJ^n}Z = \langle\psi^n\rangle \tag{3}$$

so that

$$G_1 = \frac{1}{Z}\int \psi e^{-f} = \langle\psi\rangle,$$
$$G_2^c \equiv G = Z^{-1}\int \psi^2 e^{-f} - \langle\psi\rangle^2. \tag{4}$$

While the odd correlators in the Z_2 symmetric case vanish, the exact one-body correlator is

$$G = \frac{\sqrt{\pi}}{2Zb^{3/4}}\text{Hypergeometric U}\left[\frac{3}{4}, \frac{1}{2}, \frac{a^2}{4b}\right], \tag{5}$$

where the partition function itself is

$$Z = \sqrt{\frac{a}{2b}}\exp\left[\frac{a^2}{8b}\right]\text{Bessel K}\left[\frac{1}{4}, \frac{a^2}{8b}\right]. \tag{6}$$

The dependence of the correlator on b for $a = 1$, is given in Fig. 1 as a red line.
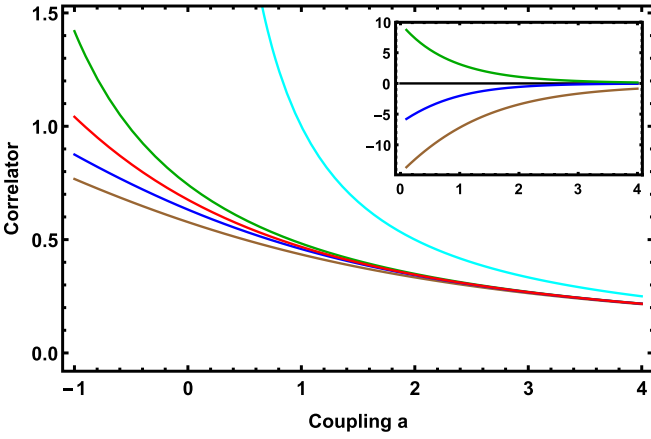
FIG. 1. Comparison of a series of successive covariant approximations for a simple integral representing in a nutshell the Z_2 symmetric statistical (or quantum many-body quantum) system. The red line is the exact correlator, while the cyan, brown, green, and blue are classical, Gaussian, cubic, and quartic approximants, respectively. Inset shows deviations (in percent) from the exact correlator.

Another important set of quantities include cumulant [20] defined via the "effective action," the Legendre transform, $A_{\text{eff}}(\psi) = F[J] + J\psi$, $\psi = -\frac{d}{dJ}F[J]$, $J = \frac{d}{d\psi}A_{\text{eff}}[\psi]$. The (two-particle irreducible) cumulants

$$\Gamma_n = \frac{d^n}{d\psi^n}A_{\text{eff}} = \frac{d^{n-1}}{d\psi^{n-1}}J. \qquad (7)$$

The well-known relations between the cumulants and correlators used below are given in Appendix A.

B. The set of the DS equations

The first in a series of the DS equations, the off-shell "equation of state" (ES, the term "off-shell" in this paper meaning that the quantity depends on the external source J) is

$$0 = -\int \frac{d}{d\psi}e^{-f} \rightarrow J = \frac{1}{Z}\int (a\psi + b\psi^3)e^{-f}$$
$$= a\psi + b\langle\psi^3\rangle. \qquad (8)$$

Using the connected correlators [20] (marked by subscript c) and eventually cumulants, one obtains

$$J = a\psi + b\psi^3 + 3b\psi G + bG_3^c. \qquad (9)$$

Higher-order DS equations in the cumulant form are obtained by differentiating the equation above. The second DS equation is

$$\Gamma = a + 3b\psi^2 + 3bG + 3b\psi\frac{d}{d\psi}G + b\frac{d}{d\psi}G_3^c$$
$$= a + 3b\psi^2 + 3bG + 3b\psi\Gamma G_3^c + b\Gamma G_4^c, \qquad (10)$$

while the next is more complicated,

$$\Gamma_3 = 6b\psi + 6b\Gamma G_3^c - 3b\psi\Gamma^3 G_3^{c2} + 3b\psi\Gamma^2 G_4^c$$
$$- b\Gamma^3 G_3^c G_4^c + b\Gamma^2 G_5^c. \qquad (11)$$

Furthermore, the fourth DS (disregarding odd condensates, as they will not be required for our purposes) has a form

$$\Gamma_4 = 6b + 9b\Gamma^2 G_4^c - b\Gamma^4 (G_4^c)^2 + b\Gamma^3 G_6^c. \qquad (12)$$

The infinite set of DS equations is not useful in practice unless a way to decouple higher-order equations is proposed. For example, one can ignore all the G_3 and G_4 terms in Eqs. (9) and (10) so that the remaining unknown variables can be solved by the two on-shell ($J = 0$) "truncated" DS equations (or equivalently the minimization equations in Gaussian variational method): the shift equation and gap equation. This simple truncation procedure called Gaussian approximation, as stated before, is not symmetry-conserving. Fortunately, a simple improvement based on Gaussian approximation, the covariant Gaussian approximation [18], includes "chain corrections" to the two-body cumulant by taking functional derivative of the off-shell (keep finite source J) shift equation with respect to φ. The chain correction is then explicitly calculated by taking derivative of the gap equation.

In the following several sections, a hierarchy of approximations defined as truncations of the DS equations as well as their variational interpretations are introduced. The CGA scheme will immediately follow when one is familiar with the classical and Gaussian approximations. Let us start with the simplest truncation: classical approximation evaluation.

C. Classical approximation

The classical approximation consists of neglecting the two and higher-body correlators in the equation of state, Eq. (9),

$$J = a\varphi + b\varphi^3, \qquad (13)$$

so that the second and higher equations are decoupled from the first. Then the "minimization equation," that is, just the on-shell ($J = 0$) ES, $a\varphi + b\varphi^3 = 0$, is solved. For $a < 0$, there are typically several solutions of this equation [21]. Here, restricting discussion here to $a > 0$, and the solution has $\varphi = 0$.

Note that despite the fact that the minimization principle involved only the one-body cumulant φ, one can still calculate the higher cumulants within the classical approximation. These are given by derivatives of the source J with respect to φ in truncated ES, Eq. (9),

$$\Gamma_{(I)} = \frac{\delta J}{\delta\varphi} = a + 3b\varphi^2 = a. \qquad (14)$$

The full correlator in momentum space is just $G_{(I)} = 1/a$. The independence on b for $a = 1$, is given in Fig. 1 as the cyan line, compared to the exact correlator (red), emphasizes the fact that the classical approximation correlator ignores the quartic term and thus might be useful (as a starting point of the "loop expansion," see Sec. IV) only at small b.

The classical minimization equation can be interpreted variationally as optimizing the free energy (1). One can do better. Why not optimize also the connected correlator G in addition to the statistical average of the field ψ? This is the Gaussian approximation idea proposed early on in the context of quantum mechanics and develop in field theory in eighties of the last century, see Ref. [22] and references therein.

D. Covariant Gaussian approximation

Now we drop in the first two DS equations all the three field cumulants (equivalently connected correlators). This leaves us with the coupled equation for the two variational parameters

$$J = a\psi + b\psi^3 + 3b\psi G^{\mathrm{tr}};$$
$$\Gamma^{\mathrm{tr}} = a + 3b\psi^2 + 3bG^{\mathrm{tr}}. \tag{15}$$

The first equation is obviously obeyed for $\psi = 0$, while the second takes a form

$$3bG^{\mathrm{tr}2} = 1 - aG^{\mathrm{tr}} \rightarrow G^{\mathrm{tr}} = \frac{-a + \sqrt{a^2 + 12b}}{6b}. \tag{16}$$

Within the covariant approximation described in detail in Ref. [18], the connected correlator $G_{(II)}$ is equal to G^{tr}. The symmetric solution exists for any a, however spurious first order transition to the "symmetry broken" solution occurs at $a_{sc} = -\sqrt{6b}$.

The dependance of the correlator for $b = 1$ on a in the range $-1 < a < 4$ is given in Fig. 1 as the brown line. It is significantly better than classical, yet underestimates the correlator up to 15%, see inset at $a = 0$. This value already approaches the spurious transition at $a_{sc} = -\sqrt{6b}$. The approximation becomes better in the perturbative region at large a, as will be discussed later.

E. The third-order (cubic) approximation

Continuing the same idea the neglect of fourth and higher correlators. The ES of state is now exact,

$$J = a\psi + b\psi^3 + 3b\psi G^{\mathrm{tr}} + bG_3^{\mathrm{tr}}, \tag{17}$$

while the next two are approximate (truncated),

$$\Gamma^{\mathrm{tr}} = a + 3b\psi^2 + 3bG + 3b\psi \Gamma^{\mathrm{tr}} G_3^{\mathrm{tr}}; \tag{18}$$

$$\Gamma_3^{\mathrm{tr}} = -G_3^{\mathrm{tr}} \Gamma^{\mathrm{tr}3} = 6b\psi + 6b\Gamma^{\mathrm{tr}} G_3^{\mathrm{tr}} - 3b\psi \Gamma^{\mathrm{tr}3} G_3^{\mathrm{tr}2}. \tag{19}$$

The first (taken on shell, $J = 0$) equations are solved by $\psi = 0$, $\Gamma_3^{\mathrm{tr}} = G_3^{\mathrm{tr}} = 0$. Then the gap equation coincides with the Gaussian, Eq. (16), with the same solution Eq. (15). However, according to the general covariant approach outlined in Ref. [18], the calculation of correlators starts with the off-shell ES, as in original definition in the second line of Eq. (7).

For example, correction to the inverse correlator is the first derivative of Eq. (17). After making the derivative

$$\Gamma_{(III)} = a + 3b\psi^2 + 3b\psi \frac{d}{d\psi} G^{\mathrm{tr}} + 3bG^{\mathrm{tr}} + b\frac{d}{d\psi} G_3^{\mathrm{tr}}, \tag{20}$$

one substitutes the truncated quantities and their derivative *on shell*:

$$\Gamma_{(III)} = a + 3bG^{\mathrm{tr}} + b\frac{d}{d\psi} G_3^{\mathrm{tr}}. \tag{21}$$

The first two terms, according to the gap equation, Eq. (18), are inverse of the truncated propagator G^{tr}, so that the cumulant can be conveniently written as

$$\Gamma_{(III)} = \Gamma^{\mathrm{tr}} + \Delta\Gamma. \tag{22}$$

In the last term, the so-called "chain" correction, $\frac{d}{d\psi} G_3^{\mathrm{tr}}$, is naturally obtained from the differentiation of the (off-shell

multiplied by $G^{\mathrm{tr}3}$) truncated third minimization equation, Eq. (19):

$$0 = \frac{d}{d\psi} G_3^{\mathrm{tr}} + 6bG^{\mathrm{tr}3} + 6bG^{\mathrm{tr}2} \frac{d}{d\psi} G_3. \tag{23}$$

Here, the general relation between cumulant and connected functions, $G^3 \Gamma_3 = G_3$, was used. Unlike the gap equation, this equation is linear, so that

$$\frac{d}{d\psi} G_3 = -\frac{6bG^{\mathrm{tr}3}}{1 + 6bG^{\mathrm{tr}2}}, \tag{24}$$

and finally

$$\Delta\Gamma = -\frac{6bG^{\mathrm{tr}3}}{1 + 6bG^{\mathrm{tr}2}}. \tag{25}$$

Now, the spurious second-order transition to a "symmetry broken" solution occurs at a lower negative value $a_{sc} = -\sqrt{12b}$ than the CGA one. This is a trend. A higher approximation symmetric phase solution works in the increasingly large portion of the parameter space. The dependance of the correlator for $b = 1$ on a in the range $-1 < a < 4$ is given in Fig. 1 as the green line. CCA now overestimates the correlator up to 10% at $a = 0$, see inset.

F. The fourth-order (quartic) approximation

The truncation is not needed now for the first two DS equations, so that the ES stays as in Eq. (17) and the gap equation takes the full form

$$\Gamma^{\mathrm{tr}} = a + 3b\psi^2 + 3bG + 3b\psi \Gamma^{\mathrm{tr}} G_3^{\mathrm{tr}}$$
$$+ 3b\Gamma^{\mathrm{tr}2} G_3^{\mathrm{tr}2} + b\Gamma^{\mathrm{tr}} G_4^{\mathrm{tr}}, \tag{26}$$

while the next two are approximate. The third will be required off-shell,

$$\Gamma_3^{\mathrm{tr}} = 6b\psi + 6b\Gamma^{\mathrm{tr}} G_3^{\mathrm{tr}} - 3b\psi \Gamma^{\mathrm{tr}3} G_3^{\mathrm{tr}2} + 3b\psi \Gamma^{\mathrm{tr}2} G_4^{\mathrm{tr}}$$
$$- b\Gamma^{\mathrm{tr}3} G_3^{\mathrm{tr}} G_4^{\mathrm{tr}}. \tag{27}$$

The last term is needed only on-shell, thus all the odd correlators can be omitted:

$$\Gamma_4^{\mathrm{tr}} = 6b + 9b\Gamma^{\mathrm{tr}2} G_4^{\mathrm{tr}} - b\Gamma^{\mathrm{tr}4} (G_4^{\mathrm{tr}})^2. \tag{28}$$

The first and the third minimization equations are still trivially satisfied as long as odd correlators vanish. The second and the fourth equations on-shell for the two even connected correlators G^{tr} and G_4^{tr}, take (upon multiplication by G^{tr} and $G^{\mathrm{tr}4}$, respectively) the "Bethe-Salpeter" form:

$$1 = aG^{\mathrm{tr}} + 3bG^{\mathrm{tr}2} + bG_4^{\mathrm{tr}}; \tag{29}$$

$$G_4^{\mathrm{tr}} = -6bG^{\mathrm{tr}4} - 9bG^{\mathrm{tr}2} G_4^{\mathrm{tr}} + b(G_4^{\mathrm{tr}})^2. \tag{30}$$

The gap equations, solved for G_4^{tr} allows to obtain a cubic equation,

$$30b^2 G^{\mathrm{tr}3} + 15abG^{\mathrm{tr}2} - (12b - a^2)G^{\mathrm{tr}} - a = 0, \tag{31}$$

for G^{tr}.

TABLE I. Weak- and strong-coupling expansions of covariant approximations for the toy model.

approximants	weak-coupling expansion	strong-coupling expansion	$b=1$	$b=4$	$b=16$
exact	$1 - 3b + 24b^2 - 297b^3 + 4896b^4$	$0.67598b^{-1/2} - 0.27153b^{-1}$			
classical (I)	$1 + 0\,b + 0\,b^2 + 0\,b^3 + 0\,b^4$	1	114	259	559
cov. Gauss (II)	$1 - 3b + 18b^2 - 135b^3 + 1134b^4$	$0.57735b^{-1/2} - 0.16667b^{-1}$	-7.2	-10.3	-12.3
cov. cubic (III)	$1 - 3b + 24b^2 - 261b^3 + 3222b^4$	$0.74231b^{-1/2} - 0.37755b^{-1}$	3.1	5.5	7.3
cov. quartic (IV)	$1 - 3b + 24b^2 - 297b^3 + 4536b^4$	$0.63246b^{-1/2} - 0.20833b^{-1}$	-2.0	-3.7	-4.9

The cumulant Γ, given by the derivative of the ES in terms of the chain $\frac{d}{d\psi} G_3^{\mathrm{tr}}$ is the same as for the cubic approximation, Eq. (24). However, the chain equation, although still linear,

$$-\frac{d}{d\psi} G_3^{\mathrm{tr}} = 6b G^{\mathrm{tr}3} + 6b G^{\mathrm{tr}2} \frac{d}{d\psi} G_3^{\mathrm{tr}}$$

$$+ 3b G^{\mathrm{tr}} G_4^{\mathrm{tr}} - b G_4^{\mathrm{tr}} \frac{d}{d\psi} G_3^{\mathrm{tr}}, \qquad (32)$$

now gives

$$\frac{d}{d\psi} G_3^{\mathrm{tr}} = 3 G^{\mathrm{tr}} \frac{2b G^{\mathrm{tr}2} + b G_4^{\mathrm{tr}}}{b G_4^{\mathrm{tr}} - 1 - 6b G^{\mathrm{tr}2}} = 3 \frac{b G^{\mathrm{tr}2} + a G^{\mathrm{tr}} - 1}{a + 9b G^{\mathrm{tr}}}. \qquad (33)$$

The cumulant now takes a form

$$\Gamma_{(IV)} = a + 3b G^{\mathrm{tr}} + 3b \frac{b G^{\mathrm{tr}2} + a G^{\mathrm{tr}} - 1}{a + 9b G^{\mathrm{tr}}}. \qquad (34)$$

Its inverse for $b = 1$ is given in Fig. 1 as the blue line over the range $-1 < a < 4$. It underestimates the exact results by just 5% at $a = 0$, as shown in the inset. The general trend is that the approximants oscillate converging the exact result. Let us now discuss the convergence of these approximations to the exact correlator, Eq. (5) and their asymptotic at weak and strong coupling.

III. TESTING THE COVARIANT APPROXIMATIONS ON STATISTICAL PHYSICS MODELS

In this section, the results of the covariant approximants outlined above are compared with exact values (or in more complicated cases numerical simulations that is known to be reliable) for the bosonic Z_2 invariant Ginzburg-Landau-Wilson models. The formalism is generalized to the lattice model of arbitrary dimension D. We start with $D = 0$.

A. Convergence of the first four approximants to the exact correlator of the bosonic toy model

The "partition function" of the toy model, used in the previous section, Eq. (2), despite having two coefficients, a and b, has just one independent parameter: $a/\sqrt{b}$. Since $b > 0$ and we first assume $a > 0$, only $a = 1$ is considered in Fig. 1. The figure indicates that the sequence of approximants converges quite fast. To make this more quantitative, let us first compare asymptotic.

At small coupling $b \ll a^2$, the expansion up to b^4 are given in Table I. One observes that the expansion is exact

to order n^{N-1}, where N is the order of the approximation. A more surprising result is that the leading incorrect term is within 10% of the correct value. For example, for the cubic approximation the b^3 coefficient is 261 compared with exact 297, the quartic approximation the b^4 coefficient is 4536 compared with exact 4896.

At strong coupling, the situation is a bit different. At any order of the expansion parameter $1/\sqrt{b}$, the coefficient converges to the exact value at large N (see values $b = 1$, 4, and 16 in Table I). The deviation from exact (given in percent) does not exceed 13% for covariant Gaussian (typical of course to numerous "mean-field" approaches), 8% for covariant cubic, and 5% for covariant quartic. Note that the deviations would increase dramatically if a noncovariant (naive or variational) version is used [18].

To conclude, increasing the rank of the covariant truncation approach increases precision at a price of more complexity. Now we consider the same ϕ^4 Ginzburg-Landau-Wilson model in higher dimensions $D > 0$. Although an exact correlator is unknown, it can be calculated numerically with practically arbitrary precision as in Ref. [18] and compared with classical, CGA, and CCA approximations.

B. Statistical mechanics of the D-dimensional ψ^4 model

The statistical physics in terms of the (real) order parameter of the Ising universality class [20,23,24] is defined by the statistical sum $Z = \exp[-A/T]$ on a hypercube lattice $r = \{r_1, \ldots, r_D\}$ $r_i = 1, \ldots, N$:

$$A = d^D \left\{ -\frac{1}{2} \sum_{r,r'} \psi_r \nabla^2_{r-r'} \psi_{r'} \right.$$

$$\left. + \sum_r \left(\frac{a}{2} \psi_r^2 + \frac{b}{4} \psi_r^4 - J_r \psi_r \right) \right\}. \qquad (35)$$

The lattice Laplacian in D dimensions is

$$\nabla^2_r = d^{-2} \sum_{i=1,\ldots,D} (\delta_{r-\widehat{i}} + \delta_{r+\widehat{i}} - 2\delta_r). \qquad (36)$$

The hopping direction is denoted [23,24] by $\widehat{i}$. Periodicity of each direction is assumed, with "lattice spacing" setting the length scale $d = 1$.

The temperature will set the energy scale $T = 1$. This can be regarded as a lattice version of the Ginzburg-Landau-Wilson action [20,23] and is a generalization of the toy model of the previous section, in that the position index r appears. In fact, we transform it to the momentum space

$$\psi_r = \frac{1}{N^{D/2}} \sum_{k_i=1}^{N} \exp\left(\frac{2\pi i}{N} k\, r\right) \psi_k, \qquad (37)$$

so that

$$A = \frac{1}{2} \sum_k \varepsilon_k \psi_k \psi_{-k} + \frac{b}{4V} \sum_{k_1 k_2 k_3} \psi_{k_1} \psi_{k_2} \psi_{k_3} \psi_{-k_1-k_2-k_3};$$

$$\varepsilon_k = \widehat{k}^2 + a; \quad \widehat{k}^2 = 4 \sum_{i=1}^{D} \sin^2\left(\frac{\pi k_i}{N}\right), \qquad (38)$$

where $V \equiv N^D$ is the number of points of the lattice.

The off-shell truncated DS equations now take a form

$$J_{-p} = \varepsilon_p \psi_{-p} + \frac{b}{V}\left(\psi_{k_1}\psi_{k_2}\psi_{-k_1-k_2-p} + 3G_{k_1 k_2}\psi_{-k_1-k_2-p} + G_{k_1 k_2, -k_1-k_2-p}\right),$$

$$\Gamma_{qp} = \varepsilon_p \delta_{q+p} + \frac{b}{V}\left(3\psi_{k_1}\psi_{-k_1-q-p} + 3G_{k_1, p+q-k_1} + 3\Gamma_{qk_1}G_{k_1 k_2 k_3}\psi_{-k_2-k_3-p}\right),$$

$$\Gamma_{qpu} = \frac{3b}{V}\left(2\psi_{-q-p-u} + \Gamma_{qk_2}G_{k_2,k_1,-k_1-p-u} + \Gamma_{uk_2}G_{k_2,k_1,-p-q-k_1} + \Gamma_{qk_2 u}G_{k_2 k_1 k_3}\psi_{-k_2-k_3-p}\right). \qquad (39)$$

Here, summations over k_1, k_2, and k_3 should understood as an Einstein summation index are assumed. Minimization equations in the symmetry unbroken phase $\psi = \Gamma_{qpu} = 0$ phase reduces to the Gaussian one, solved in Ref. [18].

The Z_2 symmetric solution of the minimization equations reduce, as in the toy model, to the solution of the gap equation, that due to translation invariance

$$\Gamma_{qp}^{\mathrm{tr}} = \delta_{q+p}\gamma_p; \quad \gamma_p = \widehat{p}^2 + m^2 \qquad (40)$$

is algebraic:

$$m^2 = a + \frac{3}{V}\sum_k g_p. \qquad (41)$$

There $g_p = \gamma_p^{-1}$. Correction to correlator subsequently is

$$\Delta\gamma_p = \frac{b}{V}\sum_{k_1 k_2} C_{-p;k_1,k_2,-p-k_1-k_2} = \frac{b}{V}\sum_{k_1 k_2} c_{p;k_1,k_2}, \qquad (42)$$

where the chain is defined as $C_{w;l_1 l_2 l_3} \equiv \frac{\delta}{\delta\psi_w} G_{l_1 l_2 l_3}$. The translation invariance of the chain, $C_{w;l_1 l_2 l_3} = \delta_{l_1+l_2+l_3-w} c_{w;l_1 l_2}$, allows to write the second equality.

Let us turn now to the chain equations, obtained, as in the toy model, from (functional) derivative of the third DS equation, Eq. (39). It reads

$$c_{w;lm} = -\frac{3b}{V}\left(2g_l g_m g_{-l-m+w} + g_m g_{-l-m+w}\sum_k c_{w;lk}\right.$$

$$\left. + g_l g_m \sum_k c_{w;-l-m+w,k}\right). \qquad (43)$$

One notices that due to locality of the interaction, in addition to the fact that w is a "spectator," on the right-hand side of the equation only the sum over the last momentum k in c appears. Since we need only summed c in the correction to the inverse correlator, Eq. (42), we sum up the equation over the last index m, $c_{w;l} \equiv \sum_m c_{w;lm}$. Using the fish integral

$f_w = \frac{1}{V}\sum_k g_k g_{w-k}$, the chain equation finally takes the form

$$c_{w;l} = -3b\left(2g_l f_{w-l} + f_{w-l}c_{w;l} + \frac{g_l}{V}\sum_k g_k c_{w;-l-k+w}\right). \qquad (44)$$

This set of V linear equations is solved numerically. Let us start with a simpler 1D case that allows a simpler solution (and can be interpreted as quantum mechanics of the anharmonic oscillator).

C. D=1 chain (or quantum mechanical anharmonic oscillator)

The $D = 1$ case corresponds to the Ginzburg-Landau-Wilson type description of the Ising chain. It is equivalent to the quantum mechanics of the anharmonic oscillator for small d limit, see Eq. (35). This case, although not solvable analytically, allows numerical solution with unlimited precision, and is compared with covariant Gaussian and cubic approximations first. A more general case of arbitrary d is compared with MC simulations.

1. Low-temperature compared with the quantum anharmonic oscillator

In 1D, the temperature T in statistical physics of classical chain can be reinterpreted as $\hbar$ and the quantum anharmonic oscillator,

$$H = -\frac{1}{2}\frac{d^2}{dx^2} + \frac{a}{2}x^2 + \frac{b}{4}x^4, \qquad (45)$$

discretized partition function (at temperature $T = 1/N$). For very large N, the correlator approaches the correlation of $x(\tau)$ for the ground state of the quantum anharmonic oscillator [23]. The thermal fluctuations in this interpretation are replaced by the quantum ones. A classical approximation and CGA for this model for the correlator and some composite correlators were worked out in Ref. [18].

The distance between spatial points should be a small as possible, so we take $d = 1/20$. The coupling b is fixed at $b=1$ (can be rescaled to this value), while $a = -1.5, -1, 0, 1$. The
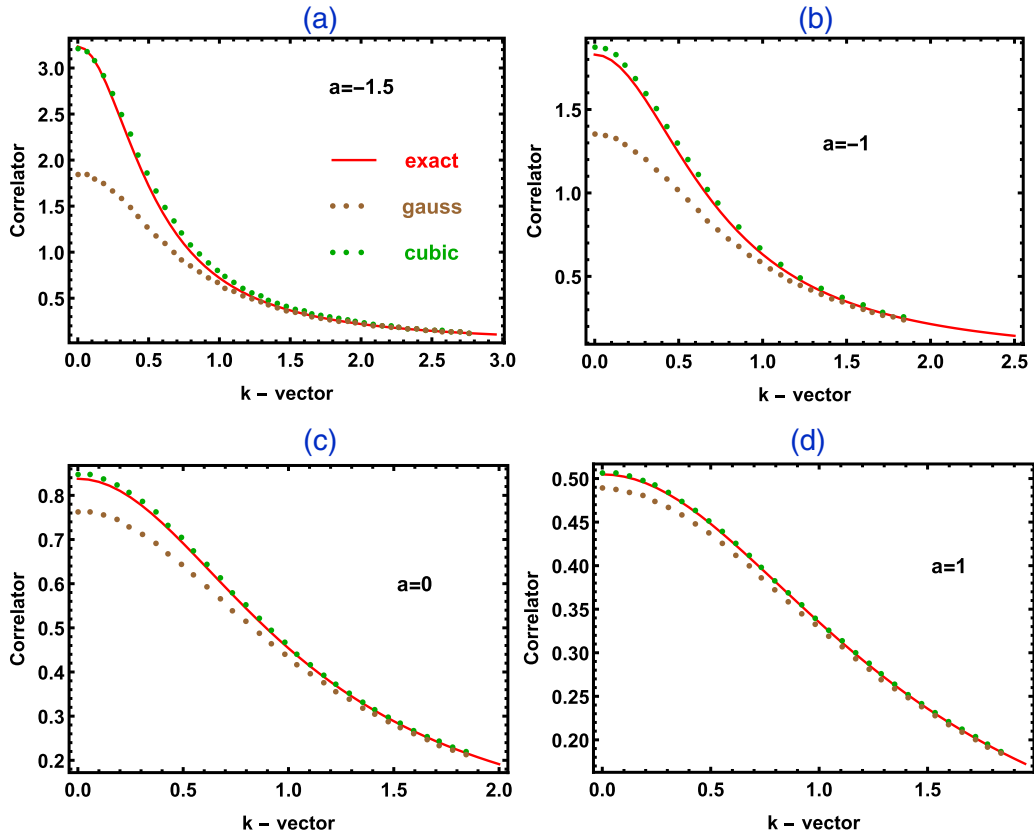
FIG. 2. Comparison of a Gaussian and cubic covariant approximations for a 1D Ginzburg-Landau-Wilson chain (representing the Z_2 symmetric statistical physics) for small $d = 1/20$ with quantum mechanical anharmonic oscillator. The red line is the exact correlator, while the brown and the green dots are CGA and CCA, respectively.

"exact" correlator (the red line in Fig. 2) was calculated as

$$G_k = |\langle 0|x|0\rangle|^2 2\pi \delta_k + \sum_{n>0} |\langle 0|x|n\rangle|^2 \frac{2(E_n - E_0)}{k^2 + (E_n - E_0)^2},$$

(46)

where E_n and $|n\rangle$ are eigenvalues and eigenstates of Hamiltonian of Eq. (45). We used $N = 2048$ to ensure continuum limit. One observes that the convergence to exact value is generally faster than in $D = 0$, see Fig. 1. Cubic overestimates much less than the Gaussian underestimates the correlator for all k vectors. For example, the $a = 1$, Fig. 2(d), CCA is within 1% for the whole range of k vectors. Even for negative values of a CCA is very precise away from the spurious phase transition of the Gaussian approximation at $s_{spt} = -1.97$. It was shown in Ref. [18] that the instanton calculus is effective only for $a < -3$, so that the approximations work in the region where no other simple approximation scheme exists. For the value of d that is not small, one cannot rely on continuum limit quantum mechanics, so the Monte Carlo approximate method is employed.

2. Monte Carlo simulation of the GLW action on finite chain

In Fig. 3, the results of the MC calculation of the average correlator in space $\langle \psi_x^2 \rangle$ are shown for a in the range -1 to 4 and $b = 1$. The sample size was $N = 256$ with $d = 1$ (with periodic boundary condition). The standard METROPOLIS algorithm is usually inefficient for $a < 0$ because of the large

autocorrelation of the samples. The autocorrelation, however, can be reduced to a large extent by combining the Metropolis algorithm with the cluster algorithm. This is done by using Wolff's single-cluster flipping method [25]. Each cycle of the MC iteration contains a single cluster update of the embedded Ising variables, followed by a sweep of local updates of the
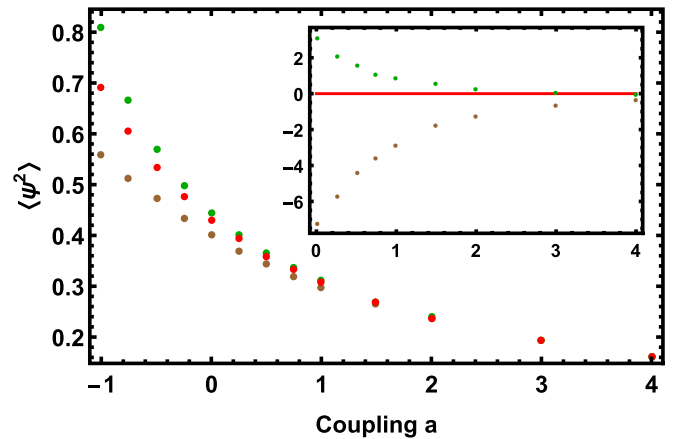

FIG. 3. Comparison of a Gaussian and cubic covariant approximations for a 1D Ginzburg-Landau-Wilson chain at $d = 1$. The red line is the MC simulation result, while the brown and the green lines are covariant Gaussian and cubic approximants, respectively. Inset shows deviations (in percent) from the exact value.
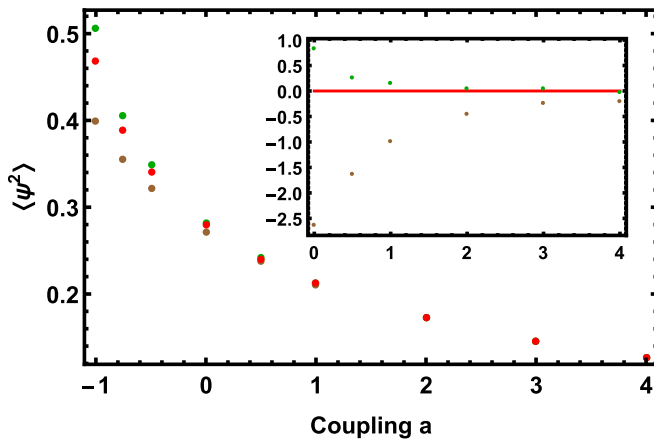
FIG. 4. The order parameter square of 2D Ginzburg-Landau-Wilson model. MC simulation results (the red dots) are compared with covariant Gaussian (the brown dots) and cubic (green dots) approximations.

original fields using Metropolis algorithm. The calculated integrated autocorrelation time was typically less then 10 second in a desktop PC. With such reduced autocorrelation, the statistical error for a run containing several 10^5 cycles after reaching equilibrium is already small enough.

The CCA was computed for the same sample size using MATHEMATICA (green dots in Fig. 3. The results are reminiscent of the quantum mechanical continuum limit with maximal deviations at $a = -1$ of 6% for CGA (underestimate) reduced to 2% for CCA (overestimate). A naive expectation is that, when dimensionality is increased or interaction that becomes longer range, the mean-field-like approximations of the type considered here, the range of applicability grows. Although in the present paper nonlocal interactions (most notably Coulomb interactions in insulators, semiconductors) are not considered here, the Ginzburg-Landau-Wilson model has been studied by MC in higher dimensions ($D = 2, 3$) [26] and it will be compared with the CCA calculation below.

D. CCA for the $D = 2$ Ginzburg-Landau-Wilson model compared to MC simulation

Similar calculation has been performed in 2D for the sample size 32×32. Here in the same region of parameter space, $-1 < a < 4$, $b = 1$, the fluctuations influence is less pronounced, so the cluster method is not required in the case not being too near the critical state. This is above the second-order phase transition (lower critical dimensionality for the Z_2 spontaneous symmetry breaking is $D = 2$) at $a_c = -1.1$ deduced from the correlator $\langle \psi_{r'} \psi_{r+r'} \rangle$ as a function of distance between the two points. The correlator was averaged over 128 points r'. Results for $\langle \psi_r^2 \rangle$ are presented (as the red dots) in Fig. 4. The precision estimate for $\langle \psi_r^2 \rangle$ is 0.2%. Thermalization was achieved after 10^5 MC steps and 3×10^5 were used for measurement.

Gaussian approximation for $\langle \psi_r^2 \rangle$ was calculated on the same lattice, see brown dots in Fig. 4. As was noticed long ago [22], the transition at $a_c = -1.198$ is a spurious weakly first order with finite excitation mass $m^2 = 0.12$ on the symmetric side (symmetric solution exists for any a). This fact was one

of the problems of the approximation at the early stages of its development. The spurious first transition, however, is very close to the second-order transition point found in MC. CGA underestimates the MC result by 2.5% at $a = 0$, see inset.

The CCA value for $\langle \psi_r^2 \rangle$ in the same range was computed for the same sample size using Mathematica (green dots in Fig. 4) using parallel computing. The results, green dots in Fig. 4, overestimate the MC value by 0.8% at $a = 0$. Of course, in the perturbative region (large a), as before the Gaussian approximation is one loop exact, while the cubic is two-loop exact. Generally, 2D convergence is better than in 1D and is expected to further improve in 3D.

In the next section, we formulate the CCA for a general fermionic model and apply it to develop a calculational scheme for a general computation of the electron Green function for an arbitrary crystalline material.

IV. COVARIANT CUBIC APPROXIMATION FOR INTERACTING ELECTRONS

Covariant Gaussian approximation for a fermionic system interacting via local four-Fermi term has been considered long time ago and compare well [17] with exact scattering matrix found by the factorization methods [27] in some $1 + 1$-dimensional relativistic models (the Gross-Neveu model, known in condensed matter physics as the Schrieffer-Su-Heeger model, was considered). Here, we formulate the third-order covariant approximation, CGA, that surprisingly turns out to be not much more complicated computationally. The additional effort is to solve large systems of linear equations.

A. Cubic approximation in general four-fermion interaction model.

Let us start with a rather general case using abstract notations, to demonstrate the general structure of the method. All the characteristics of fermionic degrees of freedom (electrons) like location in space, time, charge, band index (including spin), etc., described by (real) Grassmanian numbers are lumped into one index A. The four-Fermi interaction model (described in more detail for "down-folded" models electrons on lattice with effective interactions in the next section) is defined by the Nambu-Matsubara "action" and "statistical sum":

$$
\mathcal{A}[\psi] = \frac{1}{2} \psi^A T^{AB} \psi^B + \frac{1}{4!} V^{ABCD} \psi^A \psi^B \psi^C \psi^D;
$$
$$
Z[J] = \int D\psi \exp(-\mathcal{A}[\psi] + J^A \psi^A). \tag{47}
$$

This formalism is slightly more general than the complex Grassmanian numbers approach [28], in which a conjugate pair ψ, ψ^* is was describing annihilation or creation of a charged fermion. The Nambu approach is often used in description of superconducting state has an advantage of transparency due to explicit antisymmetry of all the Grassmanians. In particular, the "hopping amplitudes" T^{AB} and the interaction V^{ABCD} are totally antisymmetric in generalized indices.

Let us adjust the definitions of correlators to the fermionic case, paying attention to order of the Grassmanian variables and their derivatives. Cumulants and connected correlators of

fermions are defined as

$$\Gamma^{A_1 A_2 \ldots A_n} = \frac{\delta^n \mathcal{A}^{\text{eff}}}{\delta \psi^{A_1} \delta \psi^{A_2} \ldots \delta \psi^{A_n}};$$

$$G_c^{A_1 A_2 \ldots A_n} = -\frac{\delta^n F}{\delta J^{A_1} \ldots \delta J^{A_n}}$$

$$= \langle \psi^{A_1} \ldots \psi^{A_n} \rangle_c \equiv \langle A_1 \ldots A_n \rangle \qquad (48)$$

The description of CCA closely follows the steps described for bosons above. The first is "truncation" of the infinite set of DS equations.

1. First three DS equations and their truncation

Differentiating the effective action (Legendre transform of $F[J] \equiv -\ln [Z[J]]$) off-shell (namely in the presence of the

fermionic source J), the equation of motion is

$$J^A = -\frac{\delta A^{\text{eff}}}{\delta \psi_A} = -T^{AX} \psi^X - \frac{1}{3!} V^{AX_2 X_3 X_4}$$

$$\times \{ \psi^{X_2} \psi^{X_3} \psi^{X_4} + 3\psi^{X_2} \langle X_3 X_4 \rangle + \langle X_2 X_3 X_4 \rangle \}. \qquad (49)$$

Note that the antisymmetry of the coefficients in the Nambu real Grassmanian used here greatly simplifies the expressions compared to the complex Grassmanian formalism. Similarly, the second DS, using repeatedly the relation $\frac{\delta}{\delta \psi^B} \langle X_1 \ldots \rangle = \Gamma^{YB} \langle Y X_1 \ldots \rangle$, is

$$\Gamma^{AB} = \frac{\delta}{\delta \psi^B} J^A \simeq -T^{AB} - \frac{1}{2} \{ V^{ABX_3 X_4} \psi^{X_3} \psi^{X_4} + V^{ABX_3 X_4} G^{X_3 X_4} - V^{AX_2 X_3 X_4} \psi^{X_2} \Gamma^{X_1 B} \langle X_1 X_3 X_4 \rangle \}. \qquad (50)$$

As in the bosonic CCA of the previous section, the fourth correlator term was dropped from the truncated equation (this is the meaning of "$\simeq$"). Similarly, all the terms containing fourth and fifth cumulants will be dropped from the third DS equation:

$$\Gamma^{CAB} = \frac{\delta}{\delta \psi^C} \Gamma^{AB} \simeq -\frac{1}{2} \left\{ \begin{array}{c} 2V^{ABCX} \psi^X + V^{ABX_3 X_4} \Gamma^{X_1 C} \langle X_1 X_3 X_4 \rangle \\ -V^{ACX_3 X_4} \Gamma^{X_1 B} \langle X_1 X_3 X_4 \rangle + V^{AX_2 X_3 X_4} \psi^{X_2} \Gamma^{CX_1 B} \langle X_1 X_3 X_4 \rangle \end{array} \right\}. \qquad (51)$$

These equations will be used twice. First, the on-shell version, $J = 0$, the minimization equations are solved and then, the (CCA) correlator is computed from a derivative of the ES using via chain rule.

2. Minimization equations: just the Hartree-Fock approximation

In fermionic systems, one obviously does not have nonzero expectation values for (on-shell, $J = 0$) odd cumulants, namely $\langle X \rangle = \langle X_1 X_2 X_3 \rangle$ vanish on-shell. Unlike in the bosonic theories this does not hinge on the preservation of symmetries. As a consequence, the first and the third minimization equations are trivially satisfied. The gap equation on shell is (we do not mark "tr" for the variational on-shell Green function in this section for the simplicity of notation)

$$\Gamma^{AB} = -[G^{-1}]^{AB} = -T^{AB} - \frac{1}{2} V^{ABXY} G^{XY}. \qquad (52)$$

The first (matrix) equality has a sign opposite to that for bosons. The equation is just the Hartree-Fock self-consistency condition [28]. This means that the complexity of the only nonlinear operation within the CCA scheme for fermions coincides with the complexity of a presumably less precise CGA (equal for calculation of the one-body correlator to the HF approximation). The additional complexity arises only to the fact that within CCA the connected correlation does not coincides with the truncated correlator, as we have seen in the previous section and will be assessed later. Therefore we turn to the derivation of the correction $\Delta \Gamma^{AB}$ formally similar to that in the bosonic model, Eq. (22).

3. Correction to correlator

The CCA inverse correlator is a derivative of the off-shell ES, Eq. (49):

$$\Gamma_{(III)}^{AB} = \frac{\delta J^A}{\delta \psi^B} = -T^{AB} - \frac{1}{2} (V^{ABX_1 X_2} \psi^{X_1} \psi^{X_2}$$

$$+ V^{ABX_1 X_2} G^{X_1 X_2} - V^{AX_2 X_3 X_4} \psi^{X_2} \Gamma^{X_1 B} \langle X_1 X_3 X_4 \rangle)$$

$$- \frac{1}{3!} V^{AX_1 X_2 X_3} \frac{\delta}{\delta \psi^B} \langle X_1 X_2 X_3 \rangle. \qquad (53)$$

The on-shell nonzero contributions to $\Gamma_{(III)}^{AB}$ in the fermionic model are written via correction $\Gamma_{(III)}^{AB} = \Gamma^{AB} + \Delta \Gamma^{AB}$ as

$$\Delta \Gamma^{AB} = -\frac{1}{3!} V^{AX_1 X_2 X_3} \frac{\delta}{\delta \psi^B} \langle X_1 X_2 X_3 \rangle$$

$$= -\frac{1}{6} V^{AX_1 X_2 X_3} [B | X_1 X_2 X_3]. \qquad (54)$$

The first term is just the truncated inverse correlator (or the covariant Gaussian inverse correlation) in view of the gap equation, Eq. (52). The chain, a derivative of truncated three-point connected correlator will be denoted by

$$\frac{\delta}{\delta \psi^B} \langle X_1 X_2 X_3 \rangle \equiv [B | X_1 X_2 X_3]. \qquad (55)$$

The "chain" is found from the derivative of the third DS equation, Eq. (51).

4. The chain equation

Differentiating the "connected version" of the third truncated DS equation,

$$\langle Z_1 Z_2 Z_3 \rangle = G^{Z_1 Y_1} G^{Z_2 Y_2} G^{Z_3 Y_3} V^{Y_1 Y_2 Y_3 X} \psi^X$$

$$+ \frac{1}{2} V^{Y_1 Y_2 Y_3 Y_4} G^{Z_2 Y_2} G^{Z_3 Y_3} \langle Z_1 Y_1 Y_4 \rangle \qquad (56)$$

$$+ \frac{1}{2} V^{Y_1 Y_2 Y_3 Y_4} G^{Z_1 Y_1} G^{Z_2 Y_2} \langle Z_3 Y_3 Y_4 \rangle, \qquad (57)$$

one obtains on-shell:

$$
\begin{aligned}
[B|Z_1Z_2Z_3] &= G^{Z_1Y_1}G^{Z_2Y_2}G^{Z_3Y_3}V^{Y_1Y_2Y_3B} \\
&\quad + \tfrac{1}{2}V^{Y_1Y_2Y_3Y_4}G^{Z_2Y_2}G^{Z_3Y_3}[B|Z_1Y_1Y_4] \\
&\quad + \tfrac{1}{2}V^{Y_1Y_2Y_3Y_4}G^{Z_1Y_1}G^{Z_2Y_2}[B|Z_3Y_3Y_4]. \quad (58)
\end{aligned}
$$

One can prove that the chain is antisymmetric under $[B|Z_1Z_2Z_3] = -[B|Z_3Z_2Z_1]$ only. For example, $[B|Z_1Z_2Z_3] \neq -[B|Z_2Z_1Z_3]$. This is typical for "truncated" (noncovariant) quantities that was observed already in CGA [17,18].

The first important observation is that the chain equation is linear, as in the bosonic case. An additional important observation is that the parameter B is a "spectator," so, since it is an external index in the correlator itself, Eq. (54), one do not have to run over all its values.

5. Most economic linear combination of chains: V chains

The chain equations although linear are very numerous. On the other hand, a glance at the expression for the correction to the inverse correlator, Eq. (54), shows that only N linear combinations are required. A general question arises whether some linear combinations are "closed" on themselves. We have already noticed "spectators" in Eq. (58).

After some "trial and error," it turns out that the following combinations of the chains are more convenient. Defining the convenient chains combination as

$$
\langle B|AY|X_1 \rangle = V^{AYX_2X_3}[B|X_1X_2X_3], \quad (59)
$$

the correction becomes a "trace":

$$
\Delta\Gamma^{AB} = -\tfrac{1}{6}V^{AX_1X_2X_3}[B|X_1X_2X_3] = -\tfrac{1}{6}\langle B|AY|Y \rangle, \quad (60)
$$

where Y is the summation index, and Y and Z indices are also summation indices in the equation below. The "V chain" (antisymmetric in the second and third index) obeys the corresponding linear combination of the chain equations:

$$
\begin{aligned}
\langle B|X_1X_2|R \rangle &= V^{X_1X_2Z_1Z_2} \\
&\times \left\{ \begin{array}{l} \langle Z_1Y_1 \rangle \langle RY_3 \rangle \langle Z_2Y_2 \rangle V^{Y_1Y_2Y_3B} + \tfrac{1}{2}\langle Z_1Y_1 \rangle \\ \times ((\langle Z_2Y_2 \rangle \langle B|Y_1Y_2|R \rangle - \langle RY_2 \rangle \langle B|Y_1Y_2|Z_2 \rangle) \end{array} \right\}. \quad (61)
\end{aligned}
$$

This allows to solve the set of linear equations less times and in addition to use the "reduce" routines. Let us now apply the rather abstract formalism to a sufficiently general charge conserving electronic system.

B. Charge conserving electron system with pairwise interaction

1. Matsubara action

The Matsubara action of the general pairwise interacting downfolded electron model has the form [28]

$$
\begin{aligned}
\mathcal{A}[\psi] &= \psi_a^* T_{ab} \psi_{\dot{b}} + \tfrac{1}{2}\psi_a^* \psi_{\dot{a}} V_{ab} \psi_{\dot{b}}^* \psi_{\dot{b}}; \\
Z[J] &= \int D\psi D\psi^* \exp[-\mathcal{A}[\psi] + J_a^*\psi_a^* + J_{\dot{a}}\psi_{\dot{a}}].
\end{aligned} \quad (62)
$$

Charge conservation is explicit here. This should be matched with fully symmetrized Grassmanian form, Eq. (47):

$$
\mathcal{A} = \tfrac{1}{2}\psi_a^A T_{ab}^{AB}\psi_B + \tfrac{1}{4!}V_{abcd}^{ABCD}\psi_a^A\psi_b^B\psi_c^C\psi_d^D - J_a^A\psi_a^A. \quad (63)
$$

Here, $A = *, \cdot$ is the charge (Nambu) index that originate from the creation and annihilation operators in the many-body Hamiltonian [28]. The rest of the indices are contained in $a = \{$position, time, band$\}$. The "band" index includes spin. The interaction is of the density-density form and thus $V_{ab} = V_{ba}$. The result is

$$
T_{ab}^{AB} = \delta^{A*}\delta^{B\cdot}T_{ab} - \delta^{A\cdot}\delta^{B*}T_{ba}; \quad (64)
$$

$$
V_{y_1y_2y_3y_4}^{Y_1Y_2Y_3Y_4} = \left\{ \begin{array}{l} \delta_{y_3y_4}V_{y_3y_1}\delta_{y_1y_2}(\delta^{*Y_4}\delta^{\cdot Y_3} - \delta^{\cdot Y_4}\delta^{*Y_3})(\delta^{*Y_2}\delta^{\cdot Y_1} - \delta^{\cdot Y_2}\delta^{*Y_1}) \\ -\delta_{y_2y_4}V_{y_2y_1}\delta_{y_1y_3}(\delta^{*Y_4}\delta^{\cdot Y_2} - \delta^{\cdot Y_4}\delta^{*Y_2})(\delta^{*Y_3}\delta^{\cdot Y_1} - \delta^{\cdot Y_3}\delta^{*Y_1}) \\ -\delta_{y_1y_4}V_{y_3y_1}\delta_{y_3y_2}(\delta^{*Y_4}\delta^{\cdot Y_1} - \delta^{\cdot Y_4}\delta^{*Y_1})(\delta^{*Y_2}\delta^{\cdot Y_3} - \delta^{\cdot Y_2}\delta^{*Y_3}) \end{array} \right\}.
$$

This model is now amenable to the CCA approximation scheme. In the present paper, only the correlator (one body correlator or green function) is computed.

2. CCA equations for the correlator

For charge unbroken case (no superconductivity) some simplifications occur. All the "charges" correlators like G_{ab}^{**} vanish on-shell. The only correlators remaining are $G_{ab}^{*\cdot} \equiv G_{ab}$, $\Gamma_{ab}^{*\cdot} \equiv \Gamma_{ab}$, related by $\Gamma_{ax}G_{bx} = -\delta_{ab}$, where x is the summation index. General Nambu gap equation, Eq. (52) in an electric charge preserving system takes a form

$$
\Gamma_{ab} = -T_{ab} - \delta_{ab}V_{xa}G_{xx} + V_{ba}G_{ba}. \quad (65)
$$

The chain correction to the inverse propagator, Eq. (22) in our case becomes

$$
\Delta\Gamma_{ab} = \tfrac{1}{6}(\langle{}_b|_{xa}^{*}|_x^{\cdot}\rangle + \langle{}_b|_{xa}^{**}|_x^{*}\rangle). \quad (66)
$$

Only two charge components of the chain appear here due to the antisymmetry of the chain. Let us denote them as diffuson and cooperon chains in analogy to similar expressions in diagrammatic many-body physics [29]:

$$
D_{bx_1x_2r} \equiv \langle{}_b|_{x_1x_2}^{*}|_r^{\cdot}\rangle; \quad C_{bx_1x_2r} \equiv \langle{}_b|_{x_1x_2}^{**}|_r^{*}\rangle. \quad (67)
$$

For these two quantities the general chain equation, Eq. (58), closes

$$
\begin{aligned}
D_{zx_1x_2r} = {}& 2V_{y_1z}\langle x_1y_1\rangle(\langle y_1r\rangle\langle zx_2\rangle - \langle zr\rangle\langle y_1x_2\rangle)V_{x_2x_1} - 2\delta_{x_1x_2}V_{y_1z}V_{x_2y_2}\langle y_2y_1\rangle(\langle y_1r\rangle\langle zy_2\rangle - \langle zr\rangle\langle y_1y_2\rangle) \\
& + V_{x_2x_1}\big(-\langle x_1y_1\rangle\langle y_2x_2\rangle D_{zy_1y_2r} + \tfrac{1}{2}\langle x_1y_1\rangle\langle y_2r\rangle D_{zy_1y_2x_2} + \tfrac{1}{2}\langle y_1x_2\rangle\langle y_2r\rangle C_{zy_1y_2x_1}\big) \\
& + \delta_{x_1x_2}V_{x_1y_3}\big(\langle y_3y_1\rangle\langle y_2y_3\rangle D_{zy_1y_2r} - \tfrac{1}{2}\langle y_3y_1\rangle\langle y_2r\rangle D_{zy_1y_2y_3} - \tfrac{1}{2}\langle y_1y_3\rangle\langle y_2r\rangle C_{zy_1y_2y_3}\big); \\
C_{bx_1x_2r} = {}& 2V_{x_2x_1}V_{by}\langle ry\rangle(\langle bx_2\rangle\langle yx_1\rangle - \langle bx_1\rangle\langle yx_2\rangle) \\
& + V_{x_2x_1}\big(\tfrac{1}{2}\langle y_2x_1\rangle\langle ry_1\rangle D_{by_1y_2x_2} - \tfrac{1}{2}\langle y_2x_2\rangle\langle ry_1\rangle D_{by_1y_2x_1} - \langle y_2x_2\rangle\langle y_1x_1\rangle C_{by_1y_2r}\big).
\end{aligned}
\tag{68}
$$

Solution and application of these equations greatly simplifies when the translational symmetry is utilized.

3. Translation invariance

In addition to charge conservation, we assume the electronic system to be invariant under a crystalline translation symmetry and time translations. The model of relevant number of N_f bands (including spin) constructed on the lattice with periodic boundary conditions N_s in each direction, to keep notations as simple as possible, the square lattice is assumed with lattice spacing defining the unit of length $a = 1$. The points therefore are $r_i = 1, \ldots, N_s$, $i = 1, \ldots, D$ (dimensionality). At temperature T, the Matsubara (Euclidean) time is also discretized $t = 1, \ldots, N_t$ in the range $0 < \frac{1}{TN_t}t \leqslant 1/T$ and ψ_t is antiperiodic [28].

Therefore the electron field is carrying two types of indices $a = \{A, \mathbf{a}\}$, the band index will be consistently written as a superscript, while the space-time index $\mathbf{a}$ will be eventually substituted by integer valued wave number k and the Matsubara frequency n, so that we map $\psi_a \rightarrow \psi_a^{A*}$. The definitions of the discrete Fourier transform (FT) of the complex Grassmanian field is

$$
\begin{aligned}
\psi_{\mathbf{a}}^{A*} = {}& \sqrt{\frac{T}{N_s^D}}\sum_{k_1,\ldots,k_D=1}^{N_s}\sum_{n=1}^{M} \\
& \times \exp\left[-2\pi i\left(\frac{(n+1/2)t}{N_t} + \frac{k_ir_i}{N_s}\right)\right]\psi_{\alpha}^{A*}.
\end{aligned}
\tag{69}
$$

Now $\alpha = \{n, k_1, \ldots, k_D\}$ enumerates the space-time components of the energy-momentum basis. Translation invariance (energy and momentum conservation) leads to the following FT for the correlators:

$$
G_{ab}^{AB} = \frac{T}{N_s^D}\sum_{\alpha}\exp[i(\mathbf{b} - \mathbf{a})\cdot\alpha]g_{\alpha}^{AB},
\tag{70}
$$

where $\alpha = 2\pi\{\frac{(n+1/2)}{N_t}, \frac{k}{N_s}\}$. For the inverse propagator, it is convenient to define FT by

$$
\Gamma_{ab}^{AB} = \frac{\tau}{N_t N_s^D}\sum_{\alpha}\exp[i(\mathbf{a} - \mathbf{b})\cdot\alpha]\gamma_{\alpha}^{BA},
\tag{71}
$$

where $\tau = \frac{1}{TN_t}$ is the Matsubara time step, so that $g_{\alpha}^{BX}\gamma_{\alpha}^{XA} = \delta^{AB}$. Consequently, tunneling and interaction potentials FT are

$$
\begin{aligned}
T_{ab}^{AB} &= \frac{\tau}{N_t N_s^D}\sum_{\alpha}\exp[i(\mathbf{a} - \mathbf{b})\cdot\alpha]t_{\alpha}^{BA}; \\
V_{ab}^{AB} &= \frac{\tau}{N_t N_s^D}\sum_{\lambda}\exp[i(\mathbf{a} - \mathbf{b})\cdot\lambda]v_{\lambda}^{AB},
\end{aligned}
\tag{72}
$$

where $\lambda = 2\pi\{\frac{n}{N_t}, \frac{l}{N_s}\}$ has bosonic Matsubara frequency.

Using these definitions, the HF equation (65) becomes

$$
\gamma_{\alpha}^{BA} = -t_{\alpha}^{BA} - \frac{T}{N_s^D}\sum_{\chi}\big(\delta^{AB}v_0^{XA}g_{\chi}^{XX} - v_{\alpha-\chi}^{AB}g_{\chi}^{BA}\big).
\tag{73}
$$

The correction to the inverse propagator takes a form

$$
\Delta\gamma_{\alpha}^{BA} = \frac{1}{6}\frac{T}{N_s^D}\sum_{\kappa}\big(d_{\alpha\kappa\alpha}^{BXAX} + c_{\alpha\kappa\alpha}^{BXAX}\big),
\tag{74}
$$

where

$$
\begin{aligned}
D_{ax_1x_2r} &= \big(N_s^D N_t\big)^{-3}\sum_{\alpha\kappa\gamma}\exp[-(a\alpha - x_1(\kappa - \gamma) - x_2\gamma + (\kappa - \zeta)r)]d_{\alpha\kappa\gamma}; \\
C_{ax_1x_2r} &= \big(N_s^D N_t\big)^{-3}\sum_{\alpha\kappa\gamma}\exp[-(a\alpha - x_1(\kappa - \gamma) - x_2\gamma + (\kappa - \zeta)r)]c_{\alpha\kappa\gamma}.
\end{aligned}
\tag{75}
$$

Finally, the chain equations are (the spectator frequency-wave-vector indices are α and B)

$$
\begin{aligned}
c_{\alpha,\kappa,\gamma}^{BX_1X_2R} = {}& \frac{2T}{N_s^D}\Big(v_{\alpha+\chi-\gamma}^{X_1X_2}v_{\chi}^{BY}g_{\kappa-\alpha}^{RY}g_{\alpha+\chi}^{BX_2}g_{\kappa-\alpha-\chi}^{YX_1} - v_{\kappa-\alpha-\chi-\gamma}^{X_1X_2}v_{\chi}^{BY}g_{\kappa-\alpha}^{RY}g_{\alpha+\chi}^{BX_1}g_{\kappa-\alpha-\chi}^{YX_2}\Big) + \frac{T}{2N_s^D} \\
& \times \Big(v_{\alpha-\gamma-\chi}^{X_1X_2}g_{\chi+\kappa-\alpha}^{Y_2X_1}g_{\kappa-\alpha}^{RY_1}d_{\alpha,\chi,\chi+\kappa-\alpha}^{BY_1Y_2X_2} - v_{\kappa+\chi-\alpha-\gamma}^{X_1X_2}g_{\kappa+\chi-\alpha}^{Y_2X_2}g_{\kappa-\alpha}^{RY_1}d_{\alpha,\chi,\kappa+\chi-\alpha}^{BY_1Y_2X_1} - 2v_{\chi-\gamma}^{X_1X_2}g_{\chi}^{Y_2X_2}g_{\kappa-\chi}^{Y_1X_1}c_{\alpha,\kappa,\chi}^{BY_1Y_2R}\Big); \\
d_{\alpha,\kappa,\gamma}^{BX_1X_2R} = {}& \frac{2T}{N_s^D}\Big(v_{\chi-\gamma}^{X_1X_2}v_{\alpha-\chi}^{Y_1Z}g_{\chi-\kappa}^{X_1Y_1}g_{\alpha-\kappa}^{Y_1R}g_{\chi}^{BX_2} - v_{\chi-\gamma}^{X_1X_2}v_{\kappa}^{Y_1B}g_{\chi-\kappa}^{X_1Y_1}g_{\alpha-\kappa}^{BR}g_{\chi}^{Y_1X_2}\Big) \\
& + \frac{2T}{N_s^D}\delta^{X_1X_2}v_{\kappa}^{Y_1B}g_{\chi-\kappa}^{Y_2Y_1}\Big(v_{\kappa}^{X_2Y_2}g_{\alpha-\kappa}^{BR}g_{\chi}^{Y_1Y_2} - v_{\alpha-\chi}^{X_2Y_2}g_{\alpha-\kappa}^{Y_1R}g_{\chi}^{BY_2}\Big) + \frac{T}{2N_s^D}
\end{aligned}
$$

$$\times \left(-2 v_{\chi-\gamma}^{X_1 X_2} g_{\chi-\kappa}^{X_1 Y_1} g_{\chi}^{Y_2 X_2} d_{\alpha,\kappa,\chi}^{BY_1 Y_2 R} + v_{\alpha-\chi-\gamma}^{X_1 X_2} g_{\alpha-\chi-\kappa}^{X_1 Y_1} g_{\alpha-\kappa}^{Y_2 R} d_{\alpha,\chi,\alpha-\kappa}^{BY_1 Y_2 X_2} + v_{\chi-\gamma}^{X_1 X_2} g_{\chi}^{Y_1 X_2} g_{\alpha-\kappa}^{Y_2 R} c_{\alpha,\alpha-\kappa+\chi,\alpha-\kappa}^{BY_1 Y_2 X_1} \right)$$

$$+ \frac{T}{2N_s^D} \delta^{X_1 X_2} v_{\kappa}^{X_1 Y_3} \left(2 g_{\chi-\kappa}^{Y_3 Y_1} g_{\chi}^{Y_2 Y_3} d_{\alpha,\kappa,\chi}^{BY_1 Y_2 R} - g_{\alpha-\kappa-\chi}^{Y_3 Y_1} g_{\alpha-\kappa}^{Y_2 R} d_{\alpha,\chi,\alpha-\kappa}^{BY_1 Y_2 Y_3} - g_{\kappa+\chi-\alpha}^{Y_1 Y_3} g_{\alpha-\kappa}^{Y_2 R} c_{\alpha,\chi,\alpha-\kappa}^{BY_1 Y_2 Y_3} \right), \tag{76}$$

with χ being the only summation index. To test the CCA in a fermionic model, one should apply the method to an exactly solvable one. The exact solution exists for sufficiently small N_s in the case of the local-interaction Hubbard model. We therefore apply CCA to the case of Hubbard model and compare it to the exact diagonalization [32] (ED) in the case of $N_s = 1$ (quantum dot) and 1D with small finite N_s.

V. FERMIONIC BENCHMARK MODELS: QUANTUM DOT AND ONE-DIMENSIONAL HUBBARD MODEL

A. The CCA approximation in D-dimensional one band Hubbard model

1. The model, gap, and chain equations

The single-band Hubbard model is defined on the D-dimensional hypercubic lattice. The tunneling amplitude to the neighboring site in any direction $i = 1, \ldots, , D$ is denoted

in literature by t. We chose it to be the unit of energy $t = 1$. Similarly, the lattice spacing sets the unit of length $a = 1$ and $\hbar = 1$. The Hamiltonian is

$$H = \sum_{r_1,\ldots,r_D=1}^{N_s} \left[-\sum_i \left(a_r^{A\dagger} a_{r+\hat{i}}^A + \text{H.c.} \right) \right.$$

$$\left. - \mu n_r - h a_r^{A\dagger} \sigma_z^{AB} a_r^B + U n_r^{\uparrow} n_r^{\downarrow} \right]. \tag{77}$$

The chemical potential μ and the on-site repulsion energy U are therefore given in units of the hopping energy. The "band" index therefore takes two values $A, B = \uparrow, \downarrow$. The hopping direction is denoted by $\hat{i}$ as in statistical physics model [23,24] of Eq. (36). The density and its spin components are $n_r = n_r^{\uparrow} + n_r^{\downarrow}$ with $n_r^A \equiv a_r^{A\dagger} a_r^A$. External magnetic field h makes the electrons polarized. At half-filling, $\mu = \frac{U}{2}$.

The discretized Matsubara action is [28]

$$\mathcal{A} = \tau \sum_{t,r} \left\{ \begin{array}{c} \frac{1}{\tau} \left(\psi_{t+1,r}^{A*} \psi_{t,r}^A - \psi_{t,r}^{A*} \psi_{t,r}^{A*} \right) - \frac{1}{2} \sum_i \left(\psi_{t,r}^{A\dagger} \psi_{t,r+\hat{i}}^A + \psi_{t,x}^{A\dagger} \psi_{t,r-\hat{i}}^A \right) \\ - \left(\mu_H - \frac{U}{2} \right) n_r - h \psi_r^{A\dagger} \sigma_z^{AB} \psi_r^B - U \psi_{t,r}^{\uparrow*} \psi_{t,r}^{\downarrow*} \psi_{t,r}^{\uparrow} \psi_{t,r}^{\downarrow} \end{array} \right\}, \tag{78}$$

where $n_{t,r} \equiv \psi_{t,r}^{X\dagger} \psi_{t,r}^X$ and the "slice size" in antiperiodic Matsubara time is $\tau = (T N_t)^{-1}$, where T is temperature and N_t is the number of points in the compact time axis [28]. Therefore the hopping matrix in frequency-momentum space of the corresponding Matsubara action, Eq. (62) is

$$t_{n,k}^{AB} = \delta^{AB} t_{n,k} - h \sigma_z^{AB};$$

$$t_{n,k} = \frac{1}{\tau} \left[\exp \left(i \frac{2\pi (n + 1/2)}{N_t} \right) - 1 \right] - 2 \sum_i \cos \left(\frac{2\pi k_i}{N_s} \right) - \mu_H, \tag{79}$$

while the interaction is just a constant,

$$v_{nk}^{AB} = U. \tag{80}$$

The gap equation, Eq. (65), in this case takes the form

$$\gamma_\zeta^{BA} = -t_\zeta^{AB} - U \left(\delta^{AB} n^{XX} - n^{BA} \right),$$

$$n^{AB} = \frac{T}{N_s^D} \sum_\chi g_\chi^{AB}, \tag{81}$$

where the $D + 1$ dimensional notations like $\zeta = \{n, k\}$ will be used to simplify the expressions. In the range of parameters considered in the present paper the spin rotation U(1) symmetry along the z axis will be assumed unbroken. A larger $SU(2)$ symmetry appears at zero magnetic field [30], which is not discussed here since we focus initially on the "symmetry" unbroken phases. The most general ansatz is therefore $n^{\uparrow\uparrow} = n^{\uparrow}$; $n^{\downarrow\downarrow} = n^{\downarrow}$; $n^{\uparrow\downarrow} = n^{\downarrow\uparrow} = 0$.

Therefore the only two nontrivial diagonal components (denoted by $g_\zeta^{AA} \equiv g_\zeta^A$) of the truncated inverse propagator are

$$1/g_\zeta^A = -t_\zeta^A - U n^{\overline{A}}, \tag{82}$$

where the bar over the spin index means that the spin was flipped. The couple of algebraic self-consistent equations finally is

$$n^A = -\frac{T}{N_s^D} \sum_\chi \frac{1}{t_\chi^A + U n^{\overline{A}}}, \tag{83}$$

and is easily solved numerically.

The set of chain equations greatly simplified exactly as in the bosonic model since the interaction is local. One requires only coincident coordinates for the cooperon $C_{zxxr}^{ZX_1 X_2 R}$ and diffuson $D_{zxxr}^{ZX_1 X_2 R}$ defined in Eq. (67). Moreover, the remaining U(1) spin symmetry (spin along the z axis) limits the nonzero spin components. Generally, Pauli symmetry demands that for cooperon with fixed spectator spin Z, the only nonzero choice is $C = C^{ZZ\overline{ZZ}}$. For D, the symmetry leaves three

choices $D^1 = D^{ZZZZ}$, $D^2 = D^{Z\overline{Z}\overline{Z}Z}$, and $D^3 = D^{Z\overline{Z}Z\overline{Z}}$. The resulting set of chain equations in Fourier space is

$$\frac{N_s^D}{UT}c_{\zeta\kappa} = -2Ug_{\kappa-\zeta}^{\overline{Z}}g_{\kappa-\eta}^{Z}g_{\eta}^{\overline{Z}} + \frac{1}{2}g_{\kappa-\zeta+\chi}^{Z}g_{\kappa-\zeta}^{\overline{Z}}d_{\zeta\chi}^3 - \frac{1}{2}g_{\kappa-\zeta+\chi}^{\overline{Z}}g_{\kappa-\zeta}^{Z}d_{\zeta\chi}^2 - g_{\kappa-\eta}^{\overline{Z}}g_{\eta}^{Z}c_{\zeta\kappa},$$

$$\frac{N_s^D}{UT}d_{\zeta\kappa}^1 = 2Ug_{\zeta-\kappa}^{Z}g_{\eta-\kappa}^{\overline{Z}}g_{\eta}^{\overline{Z}} + \frac{1}{2}g_{\kappa-\zeta+\chi}^{\overline{Z}}g_{\zeta-\kappa}^{Z}c_{\zeta\chi} + g_{\eta-\kappa}^{\overline{Z}}g_{\eta}^{\overline{Z}}d_{\zeta\kappa}^2 - \frac{1}{2}g_{\zeta-\kappa-\chi}^{\overline{Z}}g_{\zeta-\kappa}^{Z}d_{\zeta\chi}^3,$$

$$\frac{N_s^D}{UT}d_{\zeta\kappa}^2 = g_{\eta}^{Z}g_{\kappa+\eta}^{Z}d_{\zeta\kappa}^1 - \frac{1}{2}g_{\zeta-\kappa-\chi}^{Z}g_{\zeta-\kappa}^{Z}d_{\zeta\chi}^1,$$

$$\frac{N_s^D}{UT}d_{\zeta\kappa}^3 = 2Ug_{\eta-\kappa}^{\overline{Z}}g_{\zeta-\kappa}^{\overline{Z}}g_{\eta}^{Z} + \frac{1}{2}g_{-\zeta+\kappa+\chi}^{Z}g_{\zeta-\kappa}^{\overline{Z}}c_{\zeta\chi} + \frac{1}{2}g_{\zeta-\kappa-\chi}^{\overline{Z}}g_{\zeta-\kappa}^{Z}d_{\zeta\chi}^2 - g_{\eta}^{\overline{Z}}g_{\eta+\kappa}^{Z}d_{\zeta\kappa}^3.$$

(84)

Here summation over bosonic (χ) and fermionic (η) frequencies/momenta is assumed.

The CCA correlator, Eq. (74), in this case is

$$\Delta\gamma_\zeta^{ZZ} = \frac{T}{6N_s^D}\sum_\kappa (d_{\zeta\kappa}^1 + d_{\zeta\kappa}^3 - c_{\zeta\kappa}).$$ (85)

It was calculated (using a C++ program on parallel computer cluster described below) for the cases of the toy model (quantum dot) $D = 0$ and $D = 1$ for sufficiently small N_s so that exact diagonalization is possible.

B. Fermionic toy model: quantum dot

Let us first consider an exactly solvable model of just a single site ("quantum dot"). Recently artificial systems like that with several sited Hubbard model were manifactured [31] and the experimental results were compared with exact diagonalization (ED). The space indices are absent in the $D = 0$ model, so that the space-time index α stands for the frequency after Fourier transform. The model can be solved with the result for the correlator of the up spin being

$$g_n^\uparrow = -\frac{1}{Z}\left\{\frac{1 + e^{(\mu+h)/T}}{i\pi T(2n+1) - \mu - h}\right.$$
$$\left. + \frac{e^{(\mu-h)/T} + e^{(2\mu-U)/T}}{i\pi T(2n+1) - \mu - h + U}\right\},$$
$$Z = 1 + e^{(\mu+h)/T} + e^{(\mu-h)/T} + e^{(2\mu-U)/T}.$$ (86)

This is presented as a red lines in Fig. 5. In Fig. 5(a), the real part of the Matsubara correlator in wide range of doping $\delta\mu \equiv \mu - U/2$ for $U = 3$ is given, while Fig. 5(b) exhibits the imaginary part. Temperature and magnetic field were fixed at $T = 1$ and $h = 1$. One observes a very good agreement not only in perturbative domains for large absolute value of $\delta\mu$ (far away from half-filling). The maximal deviations are 0.03, 0.01 (real part) and 10%, 5% (imaginary part) for CGA and CCA, respectively, see insets. In Fig. 6, the same is given for a strong coupling $U = 5$. The agreement is worse, by still have maximal deviations are 0.04, 0.025 (real part) and 28%, 14% for CGA and CCA.

C. Comparison of results with exact diagonalization for one-dimensional Hubbard model

The one-dimensional case is considered for simplicity and availability of exact results utilizing the exact diagonalization [32] for reasonably large values of N_s. The largest lattice we have used to exactly calculate Green's function was $N_s = 6$ (so that the number of fermionic degrees of freedom is 12) and avoided using the Lancos algorithms to diagonalize large matrices, since temperature range $T = 0.2$–4 in units of the hopping parameter t of the Hubbard model is considered. The relatively high temperature allows lower $N_t = 512$–2048 to obtain precision of 0.2% for the CCA calculation using the "naive" discretization of Eq. (78). Larger lattices were treated by the exact diagonalization, however, in these calculations typically only spectrum and expectation values were com-
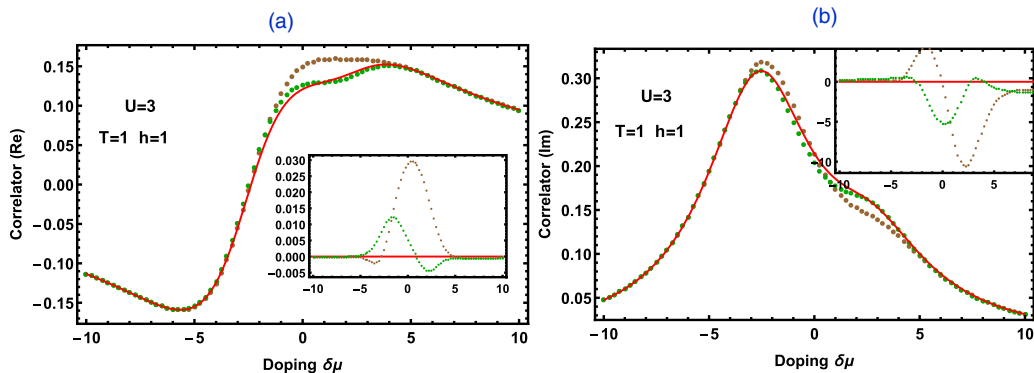

FIG. 5. Real (a) and imaginary (b) parts of the Matsubara correlator for quantum dot at intermediate value of the coupling.
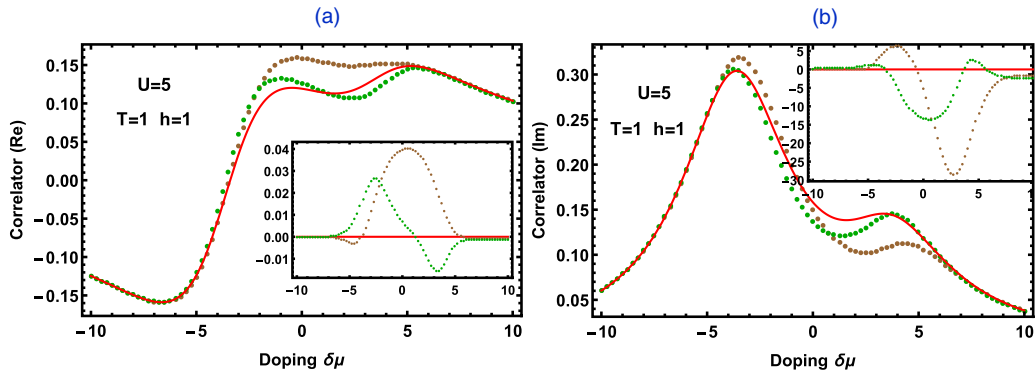
FIG. 6. Same as Fig. 5 for a rather strong coupling.

puted. To compare with CCA, the Matsubara time correlators are required. These are more difficult to compute. The program was written in Mathematica.

The program for CCA was written in C++ and utilizes parallel computing on a 128 node cluster and large memory of 512 Gbyte. The doping range was $10 < \delta\mu \equiv \mu - U/2 < 10$ for the band with 4 (in units of the hopping parameter). Temperature and magnetic field were fixed at $T = 1$, $h = 1$. The results for $N_s = 4$ are presented in Figs. 7 and 8 for intermediate, $U = 3$ and strong, $U = 5$, couplings respectively. Figures 7(a) and 8(a) show the real part of the Matsubara correlator, while Figs. 7(b) and 8(b) the imaginary part. One observes a very good agreement not only in perturbative domains for large absolute values of $\delta\mu$ (far away from half-filling). The maximal deviations are 0.013, 0.003 (real part) and 12%, 5% (imaginary part) for CGA and CCA, respectively, for $U = 3$, see insets in Fig. 7. In Fig. 8, the same is given for a strong coupling for $U = 5$. The agreement is worse, the maximal deviations are 0.02, 0.01 (real part) and 28%, 17% for CGA and CCA. Generally, results are similar to that in $D = 0$ for the relatively low value of $N_s = 4$.

Till now, the application of CCA to a number of solvable field theoretical models was considered to gauge its precision and complexity. It is not the purpose of the present paper to apply the method to a realistic material, however, below we estimate the mathematical/computational complexity of such a calculation.

VI. DISCUSSION AND CONCLUSIONS

To summarize, we have developed the covariant cubic approximation, CCA, determining the excitation properties of lattice models of electronic systems. It was shown that truncation of the set of Dyson-Schwinger equations for correlators of the model lead to a converging series of approximates. The covariance ensures that all the Ward identities expressing the charge conservation or high-order correlator identities (obtained by successive functional derivative of the Dyson equations) are obeyed. A large number of solvable bosonic and fermionic field theoretical models demonstrate that the third approximant in this series, CCA, is sufficiently precise. Moreover, it turns out that is still calculable by currently available calculational tools.

Now, let us speculate on the application of the method to crystalline solids. Although the basic band structure of crystalline solids can be theoretically investigated by the density functional methods, the condensed matter characteristics dependent on the detailed structure of the electronic matter near the Fermi level requires more precise treatment of the electrons near the Fermi level. It is not possible to perform the CCA computation for the realistic materials on the microscopic level due to complexity of the chain equations. Therefore one should rely on "downfolding" of the original microscopic Hamiltonian to a simpler interacting electronic model of Sec. IV (by "integrating out" the bands far from the Fermi surface [33]) on the sufficiently coarse grained lattice. The hopping amplitude $T^{AB}(\omega, p)$ is a function of
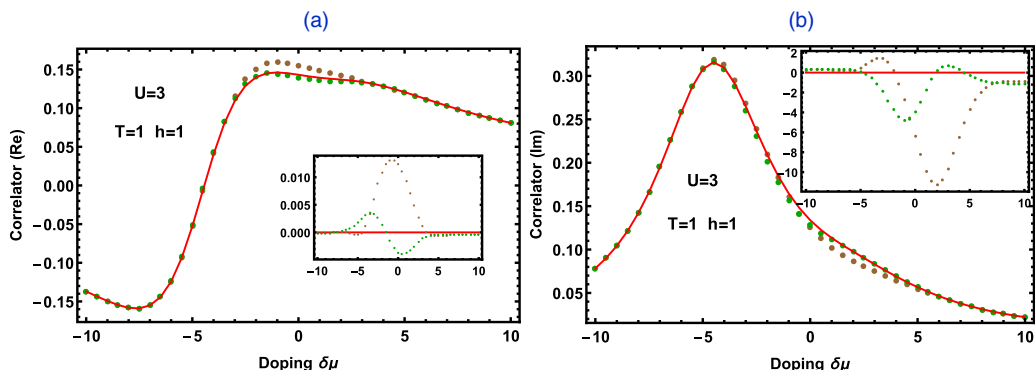

FIG. 7. Real (a) and imaginary (b) parts of the Matsubara correlator for the Hubbard spin chain at intermediate coupling.
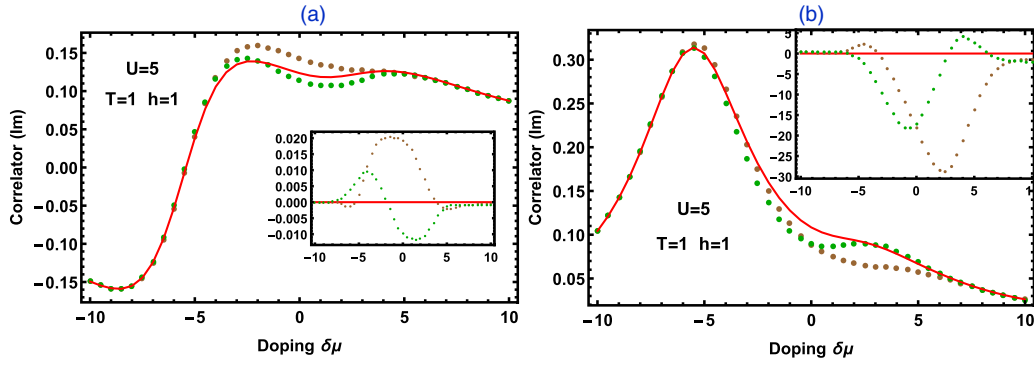
FIG. 8. Same as Fig. 7 for a larger value of the coupling.

frequency and quasimomentum with relevant bands indexed by $A = 1, \ldots, N_b$. The problem of the determination of the electromagnetic, thermal, and other condensed matter properties that incorporate the excitation effects, is divided into steps depicted in Fig. 9. The Matsubara frequency correlator calculated within CCA should therefore be analytically continued [34] to the spectral weight and density of states to be compared with experiments and other methods, see Fig. 9.

Naive estimate of the computational complexity of covariant third-order approximation is misleading due to the following three observations of the formalism presented in Sec. IV. (1) Since the odd order fermionic correlators vanish, the only variational parameter is still the truncated correlator, namely, the most complicated third equation, Eq. (56), is trivially satisfied in the fermionic model (unlike in the bosonic model in the symmetry broken phase, which is indeed too complicated). Moreover, the only on shell equation coincides with HF. (2) The chain equations (75) are all linear. We do not have a proof, but it seems to be a common feature for both covariant Gaussian and CCA. (3) The chain equations, albeit linear have a lot of variables and one can either apply a solution algorithm or look for a convergent recursion. At least in the Hubbard-type models such a recursion exists.

Let us estimate the complexity for the case of negligible spin-orbit interaction, and provide numbers using an example of a simple 2D semiconductor hexagonal 2D boron nitride, layer hBN. In this case, one can retain eight bands, $N_b = 8$, four for the boron atom and two for the nitrogen. The Brillouin

FIG. 9. Flow chart of the CCA calculation of the electron field correlator of crystalline material.

zone hexagonal grid contains N_s for $N_s = 6 \times 6$, while the number of Matsubara frequencies is $N_t = 64$. The later determines the lattice size for periodic boundary conditions and is related to physical frequencies. The number of fermionic variables in the Matsubara action is

$$n = N_s N_t N_b. \tag{87}$$

Therefore one has to solve n nonlinear equations (65). For hBN, the number of equations is $n = 3.6 \times 10^4$. Therefore generally there is no problem with either memory of the calculation time for this simple case.

The price to pay is that in addition to computing the HF fermionic Green's function, one also has to solve an extensive system of linear equations, the so-called chain equations, either in the configuration space, Eq. (68), or frequency-k-vector space, Eq. (76). The chain correction is then added to the inverse Green's function that is inherently charge conserving. The number of "chains" after reductions due to translation symmetry is very large. The number of variables in the chain equations, Eq. (76), is

$$n_{ch} = 4N_b^3 N_s^2 N_t^2. \tag{88}$$

The factor 4 is due to two "charge" and spin channels (cooperon and diffuson). In the hBN example, it amounts for the spin symmetric case to $n_{ch} = 5.4 \times 10^9$. However, the matrix is sparse, since there is only one space and time summation in the chain equation, Eq. (76). The density of the matrix (ratio of nonzero matrix elements of the total n_{ch}^2) is

$$\text{density} = \frac{1}{N_t N_s}. \tag{89}$$

This amounts to 4.3×10^{-4}, so that the matrix is sparse with 2.3×10^6 nonzero elements. This is achievable, as recent computation [35] (in a different field) with similar parameters confirms. Of course, symmetries sometimes reduce the number. The matrices are sparse in the configuration space, Eq. (68), since coefficients contain many fast decreasing Matsubara correlators. We have not made use of this calculations, preferring the exact solution. However, in realistic calculations, one might have to use a properly constructed iteration scheme. To calculate the whole set of frequencies (required for the analytic continuation) and k vectors, the equations should be solved n times ("spectator" parameter in the CCA scheme, see Sec. IV). Other methods, like iteration (using fast Fourier transforms), might be much faster.
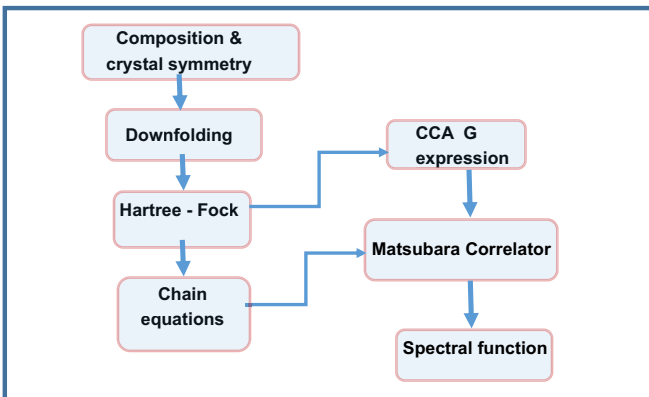
[1] P. Hohenberg and W. Kohn, Phys. Rev. **136**, B864 (1964); W. Kohn and L. J. Sham, *ibid.* **140**, A1133 (1965).

[2] G. Kotliar, S. Y. Savrasov, K. Haule, V. S. Oudovenko, O. Parcollet, and C. A. Marianetti, Rev. Mod. Phys. **78**, 865 (2006).

[3] L. Hedin, Phys. Rev. **139**, A796 (1965).

[4] S. Y. Savrasov, G. Resta, and X. Wan, Phys. Rev. B **97**, 155128 (2018).

[5] M. S. Hybertsen and S. G. Louie, Phys. Rev. Lett. **55**, 1418 (1985); F. Aryasetiawan and O. Gunnarsson, Rep. Prog. Phys. **61**, 237 (1998).

[6] J. Luttinger and J. Ward, Phys. Rev. **118**, 1417 (1960).

[7] G. Baym and L. P. Kadanoff, Phys. Rev. **124**, 287 (1961); G. Baym, *ibid.* **127**, 1391 (1962).

[8] B. Holm and U. von Barth, Phys. Rev. B **57**, 2108 (1998); A. Stan, N. E. Dahlen, and R. Van Leeuwen, Europhys. Lett. **76**, 298 (2006); J. Chem. Phys. **130**, 114105 (2009).

[9] A. Kutepov, S. Y. Savrasov, and G. Kotliar, Phys. Rev. B **80**, 041103 (2009); A. Kutepov, K. Haule, S. Y. Savrasov, and G. Kotliar, *ibid.* **85**, 155129 (2012).

[10] H. van Hees and J. Knoll, Phys. Rev. D **66**, 025028 (2002).

[11] A. L. Kutepov, J. Phys.: Condens. Matter **27**, 315603 (2015).

[12] A. L. Kutepov, Phys. Rev. B **94**, 155101 (2016); A. L. Kutepov and G. Kotliar, *ibid.* **96**, 035108 (2017).

[13] A. Gruneis, G. Kresse, Y. Hinuma, and F. Oba, Phys. Rev. Lett. **112**, 096401 (2014); E. Maggio and G. Kresse, J. Chem. Theory Comput. **13**, 4765 (2017).

[14] Y. Takada, Phys. Rev. Lett. **87**, 226402 (2001); H. Maebashi and Y. Takada, Phys. Rev. B **84**, 245134 (2011).

[15] A. Kovner and B. Rosenstein, Phys. Rev. D **39**, 2332 (1989).

[16] B. Rosenstein and A. Kovner, Phys. Rev. D **40**, 504 (1989); **40**, 515 (1989); Q. Li, D. Tu, and D. Li, Phys. Rev. A **85**, 033609 (2012); Y.-H. Zhang and D. Li, *ibid.* **88**, 053604 (2013).

[17] B. Rosenstein and A. Kovner, Phys. Rev. D **40**, 523 (1989).

[18] J. F. Wang, D. P. Li, H. C. Kao, and B. Rosenstein, Ann. Phys. **380**, 228 (2017).

[19] B. Rosenstein and D. Li, Rev. Mod. Phys. **82**, 109 (2010).

[20] D. J. Amit, Field Theory, *the Renormalization Group, and Critical Phenomena* (World Scientific, Singapore, 1984); P. M. Chaikin and T. C. Lubensky, *Principles of Condensed Matter Physics* (Cambridge University Press, Cambridge, England, 1995).

[21] For negative a, the exact expression takes a slightly different form. Negative a leads to the field reflection ($\psi \rightarrow -\psi$) Z_2-spontaneously broken solutions in the classical and sometimes Gaussian approximation. Despite the fact that we know there is no spontaneous symmetry breaking in $d = 0$, a rather precise approximation scheme for a Z_2 invariant quantity emerges when one of the two "would be" symmetry broken solutions, $\varphi = \pm\sqrt{-a/b}$, is often considered in the intermediate steps. While in a rather more comprehensive description of covariant Gaussian approximation in Ref. [18], the focus has been also on the symmetry broken phases, in the present work the emphasis will be on detailed structure of the "two-body" correlator in the symmetry preserved phase.

[22] P. M. Stevenson, Phys. Rev. D **23**, 2916 (1981).

[23] H. Kleinert, *Path Integrals in Quantum Mechanics, Statistics, Polymer Physics, and Financial Markets* (World Scientific, Singapore, 2009).

[24] H. J. Rothe, *Lattice Gauge Theories: An Introduction*, World Scientific Lecture Notes in Physics (World Scientific, Singapore, 2012).

[25] R. C. Brower and P. Tamayo, Phys. Rev. Lett. **62**, 1087 (1989); U. Wolff, *ibid.* **62**, 361 (1989).

[26] P. Arnold and G. D. Moore, Phys. Rev. E **64**, 066113 (2001).

[27] A. Zamolodchikov and Al. Zamolodchiko, Ann. Phys. (NY) **120**, 253 (1979).

[28] J. W. Negele and H. Orland, *Quantum Many-particle Systems* (Benjamin, Redwood City CA, 1988).

[29] E. Akkermans and G. Montambaux, *Mesoscopic Physics of Electrons and Photons* (Cambridge University Press, Cambridge, England, 2011).

[30] V. E. Korepin and F. H. L. Essler, *Exactly Solvable Models of Strongly Correlated Electrons* (World Scientific, Singapore, 1994).

[31] T. Hensgens, T. Fujita, L. Janssen, X. Li, C. J. Van Diepen, C. Reichl, W. Wegscheider, S. Das Sarma, and L. M. K. Vandersypen, Nature (London) **548**, 70 (2017).

[32] A. Weisse and H. Fehske, Exact Diagonalization Techniques, in *Computational Many-Particle Physics*, edited by H. Fehske, R. Schneider, and A. Weisse (Springer, Berlin, 2008).

[33] P. Werner and M. Casula, J. Phys.: Condens. Matter **28**, 383001 (2016); H. Zheng, H. J. Changlani, K. T. Williams, B. Busemeyer, and L. K. Wagner, Front. Phys. **6**, 43 (2018).

[34] M. Jarrell and J. E. Gubernatis, Phys. Rep. **269**, 133 (1996).

[35] V. Puzyrev, S. Koric, and S. Wilkin, Comput. Geosci. **89**, 79 (2016).